Numerical Investigation of Transformation Field Analysis for Elastic-Plastic Periodic Materials

Christiano A. F. Várady Filho[1], Márcio A. A. Cavalcante[2]

[1]*Centro de Tecnologia, Universidade Federal de Alagoas*
Lourival Melo Mota Av., Maceió, Brazil
christiano_varady@lccv.ufal.br
[2]*Campus de Engenharias e Ciências Agrárias, Universidade Federal de Alagoas*
Rio Largo, Brazil
marcio.cavalcante@ceca.ufal.br

Abstract. Present work analyzes the numerical cost-benefit ratio of Dvorak's Transformation Field Analysis to evaluate elastoplastic behavior of periodically perforated metal sheets. The accuracy measurement and the processing time are analyzed by implementing a finite element approach integrated with the Transformation Field Analysis technique for different meshes and finite element orders. Numerical studies are employed to compare with standard Finite Element Analysis for elastoplastic analysis of periodically perforated metal sheets. The numerical results show the technique's capabilities and favorable scenarios, besides the influence of domain discretization and finite element order.

Keywords: Transformation Field Analysis, Perforated Metal Sheets, Finite Element Method, Computational Performance.

1 Introduction

Micromechanics of porous materials assesses the influence of the porous's geometrical configuration and mechanical properties of the matrix material by homogenization and multiscale techniques. Determination of the homogenized inelastic response of porous materials integrated into a multiscale analysis continues to challenge researchers because of the complex microstructure stress and inelastic strain fields.

Those techniques are alternatives to the Finite Element Method (FEM) for mechanical analysis of periodic media. The increase in sophistication of the models and evaluation of localized phenomena requires refined discretized domains or higher-order finite elements. Some techniques address the classical Finite Element Analysis (FEA) to enhance performance. The Transformation Field Analysis (TFA) is one of them [1]. The TFA solves the non-linear analysis by adding fundamental solutions based on the concepts of concentration and influence tensors borrowed from the micromechanics analysis and applying the superposition principle.

The TFA is a procedure that decomposes the elastic strain field in a superposition of uniform eigenstrain fields, exploiting the dependence of the subdomains displacement fields and its influence in the global field [1]. The TFA relates thermal and mechanical loadings even when the phases' properties depend on the temperature variation [2]. In the TFA approach, Dvorak proposes reducing the number of calculated variables, optimizing the cost-benefit ratio of the simulation.

The superposition-based formulation can also be found in Dvorak [3], where uniform fields in a biphasic medium can be assessed. In this work, the authors calculate the influence tensors based on unit eigenstrains and define their relations with inelastic strains, considering an arbitrary geometry for the phases. They also restrict the type of inclusions where uniform strain fields are available. Additionally, Benveniste and Dvorak [4] makes some observations of the uniform field in composite materials. In the same year, Dvorak [5] expanded the formulation for multi-phase composites, and a FEM-based approach for TFA is proposed in Dvorak et al. [6], wherein the first comparison of classic FEA and TFA is investigated, and TFA shows good accuracy.

This investigation addresses the second challenge, analyzing the performance of the TFA-based Finite Ele-

ment approach for elastoplastic analysis of periodic porous media. Evaluation of numerical case studies appraise accuracy and computational cost for different discretizations, considering *h* and *p* refinements in FEA to assess favorable scenarios for applying the technique.

2 Homogenization of Periodic Materials

Mechanical analysis of periodic materials under homogeneous loading is defined by the behavior of the repeating unit cell, which consists of the pattern used to generate the whole material. The solution of the boundary-value problem subject to periodic traction and displacement boundary conditions defines the macroscale response of the material [7].

The unit cell should be well enough discretized to capture the microstructural details. Also, the displacement field in subdomains is expressed in terms of macroscopic and local contributions using a two-scale expansion in global and local coordinates,

$$u_i^{(q)}(\mathbf{x},\mathbf{y}) = \overline{\varepsilon}_{ij}x_j + \tilde{u}_i^{r(q)}(\mathbf{y}),\ i = 1,2,3 \tag{1}$$

where $\overline{\varepsilon}_{ij}$ is the macroscopic strain field applied to the entire material and $\tilde{u}_i^{r(q)}(\mathbf{y})$ is the local fluctuating displacement in the qth subdomain for the rth phase. Accordingly, the strain field is also decomposed into average and fluctuating parts $\varepsilon_i^{(q)}(\mathbf{x},\mathbf{y}) = \overline{\varepsilon}_{ij} + \tilde{\varepsilon}_{ij}^{r(q)}(\mathbf{y})$. FEA solution produces a set of equations for the parameters defining the subdomain fluctuating displacement field of the form

$$\mathbf{K}\tilde{\mathbf{u}} = \Delta\mathbf{C}\overline{\boldsymbol{\varepsilon}} + \mathbf{G}\left(\int_{V(q)} \boldsymbol{\varepsilon}^{p(q)} dV\right) \tag{2}$$

with $\Delta\mathbf{C}$ having terms of the differences in the stiffness matrix, $\mathbf{G}$ contains volume integrals of the unknown plastic strains over the subdomains and $\tilde{\mathbf{u}}$ represent nodal fluctuating displacements that are common to adjacent subdomains, which depends only on the plastic strain field $\boldsymbol{\varepsilon}^{p(q)}$.

Solution of the system, coupled with homogeneous displacement field, determines the displacement in each subdomain, wherein the volume-averaged strain in the qth subdomain can be evaluated as

$$\overline{\boldsymbol{\varepsilon}}^{(q)} = \mathbf{A}^{(q)}\overline{\boldsymbol{\varepsilon}} + \mathbf{D}^{(q)} \tag{3}$$

with $\mathbf{A}^{(q)}$ and $\mathbf{D}^{(q)}$ as the elastic strain concentration tensors [8] and inelastic influence tensors, respectively. Based on these definitions, using subdomain stresses and strains through local constitutive equations

$$\boldsymbol{\sigma}^{(q)} = \mathbf{C}^{(q)}\left(\boldsymbol{\varepsilon}^{(q)} - \boldsymbol{\varepsilon}^{p(q)}\right) \tag{4}$$

we can evaluate the volume-averaged stress in terms of the volume-averaged subdomain stress

$$\overline{\boldsymbol{\sigma}} = \frac{1}{V}\sum_{q=1}^{N_q}\int_{V_q}\boldsymbol{\sigma}^{(q)}dV = \sum_{q=1}^{N_q} c_{(q)}\overline{\boldsymbol{\sigma}}^{(q)} = \sum_{q=1}^{N_q} c_{(q)}\mathbf{C}^{(q)}\left(\overline{\boldsymbol{\varepsilon}}^{(q)} - \overline{\boldsymbol{\varepsilon}}^{p(q)}\right) = \mathbf{C}^*\left(\overline{\boldsymbol{\varepsilon}} - \overline{\boldsymbol{\varepsilon}}^{p}\right) \tag{5}$$

which is the homogenized Hooke's law. The homogenized stifness matrix $\mathbf{C}^*$ and plastic strain $\overline{\boldsymbol{\varepsilon}}^{p(q)}$ can be evaluated as

$$\mathbf{C}^* = \sum_{q=1}^{N_q} c_{(q)}\mathbf{C}^{(q)}\mathbf{A}^{(q)} \tag{6}$$

$$\overline{\boldsymbol{\varepsilon}}^{p} = [\mathbf{C}^*]^{-\mathbf{1}}\sum_{q=1}^{N_q} c_{(q)}\mathbf{C}^{(q)}\left(\overline{\boldsymbol{\varepsilon}}^{p(q)} - \mathbf{D}^{(q)}\right) \tag{7}$$

where $\overline{\boldsymbol{\varepsilon}}^{p(q)}$ is the volume-averaged plastic strains in the qth subdomain.

2.1 Transformation Field Analysis

Eigenstrains, from which TFA is based, is a mathematical concept and can represent some physical phenomenon in the manufacture or operation of composite materials caused by thermal changes, variations in the humidity of the phase material, or inelastic strains. It is essential to point out that the strains caused by stresses superior to the material's yield stress can be decomposed into its elastic and inelastic parts, and only the latter is an eigenstrain. Also, for an incremental increase in the stress field, changes in the inelastic strain field depend on the loading history.

The presence of eigenstrain $\boldsymbol{\mu}^{(r)}$ and eigenstress $\boldsymbol{\lambda}^{(r)}$ in the rth phase affects the constitutive relationships as follows

$$\boldsymbol{\sigma}^{(r)} = \mathbf{C}^{(r)}\boldsymbol{\varepsilon}^{(r)} + \boldsymbol{\lambda}^{(r)} \leftrightarrow \boldsymbol{\varepsilon}^{(r)} = \mathbf{S}^{(r)}\boldsymbol{\sigma}^{(r)} + \boldsymbol{\mu}^{(r)} \tag{8}$$

$$\text{where } \boldsymbol{\lambda}^{(r)} = -\mathbf{C}^{(r)}\boldsymbol{\mu}^{(r)} \text{ and } \boldsymbol{\mu}^{(r)} = -\mathbf{S}^{(r)}\boldsymbol{\lambda}^{(r)} \tag{9}$$

$$\therefore \boldsymbol{\sigma}^{(r)} = \mathbf{C}^{(r)}[\boldsymbol{\varepsilon}^{(r)} - \boldsymbol{\mu}^{(r)}] \leftrightarrow \boldsymbol{\varepsilon}^{(r)} = \mathbf{S}^{(r)}[\boldsymbol{\sigma}^{(r)} - \boldsymbol{\lambda}^{(r)}]\,. \tag{10}$$

An interesting way of representing the local stress/strain fields in a heterogeneous media is to employ transformation variables with uniform distributions, as proposed in Dvorak [3]. Thus, the volume-averaged strain and stress in the rth phase can be evaluated as follows

$$\overline{\boldsymbol{\varepsilon}}^{(r)} = \mathbf{A}^{(r)}\overline{\boldsymbol{\varepsilon}} + \sum_{s=1}^{N}\mathbf{D}^{(r,s)}\overline{\boldsymbol{\mu}}^{(s)} \text{ and } \overline{\boldsymbol{\sigma}}^{(r)} = \mathbf{B}^{(r)}\overline{\boldsymbol{\sigma}} + \sum_{s=1}^{N}\mathbf{F}^{(r,s)}\overline{\boldsymbol{\lambda}}^{(s)} \tag{11}$$

where $\mathbf{A}^{(r)}$ and $\mathbf{B}^{(r)}$ are the strain and stress concentration tensors for the rth phase, respectively. The tensors $\mathbf{D}^{(r,s)}$ and $\mathbf{F}^{(r,s)}$ are called transformation influence tensors for strain and stress, respectively. They measure the strain/stress in the rth phase caused by uniform eigenfields $\overline{\boldsymbol{\mu}}^{(s)}$ and $\overline{\boldsymbol{\lambda}}^{(s)}$ in the sth phase applied in a model where $\overline{\boldsymbol{\varepsilon}} = \mathbf{0}$ and $\overline{\boldsymbol{\sigma}} = \mathbf{0}$, respectively. The influence tensors $\mathbf{D}^{(r,r)}$ and $\mathbf{F}^{(r,r)}$ indicate self-induced influences in the analysis. In biphasic materials (matrix and inclusions of the same type of material), the influence tensors can be calculated as

$$\mathbf{D}^{(r,m)} = \left(\mathbf{I} - \mathbf{A}^{(r)}\right)\left(\mathbf{C}^{(m)} - \mathbf{C}^{(i)}\right)^{-1}\mathbf{C}^{(m)} \tag{12}$$

$$\mathbf{D}^{(r,i)} = -\left(\mathbf{I} - \mathbf{A}^{(r)}\right)\left(\mathbf{C}^{(m)} - \mathbf{C}^{(i)}\right)^{-1}\mathbf{C}^{(i)} \tag{13}$$

$$\mathbf{F}^{(r,m)} = \left(\mathbf{I} - \mathbf{B}^{(r)}\right)\left(\mathbf{S}^{(m)} - \mathbf{S}^{(i)}\right)^{-1}\mathbf{S}^{(m)} \tag{14}$$

$$\mathbf{F}^{(r,i)} = -\left(\mathbf{I} - \mathbf{B}^{(\mathbf{r})}\right)\left(\mathbf{S}^{(m)} - \mathbf{S}^{(\mathbf{i})}\right)^{-1}\mathbf{S}^{(i)} \tag{15}$$

for $r = m, i$.

Transformational influence tensors have emerged as an alternative for evaluating inelastic behavior caused by different types of loads. Coupling with Finite Element Analysis (displacement formulation) involves the evaluation of strain concentration and influence tensors for each finite element. The main advantage is that these tensors are evaluated just once, allowing for inelastic analysis in various situations (different loadings).

2.2 Elastoplastic Analysis

Evaluation of the elastic strain concentration and plastic influence tensors permits calculation of the homogenized elastic-plastic behavior of a periodic material for all loading steps. Assessment of the mechanical behavior is done by successive integrations in incremental form of the homogenized plastic strains using the localization equations. The homogenized plastic strain increment is given as

$$d\overline{\boldsymbol{\varepsilon}}^{p} = \sum_{e=1}^{N_e} c_{(e)}\mathbf{B}^{(e)}d\overline{\boldsymbol{\varepsilon}}^{p(e)} \tag{16}$$

where the elastic stress concentration tensor is evaluated by $\mathbf{B}^{(e)} = [\mathbf{C}^*]^{-1} \left[\mathbf{A}^{(e)}\right]^T \mathbf{C}^{(e)}$ and the local plastic strain increment $d\bar{\boldsymbol{\varepsilon}}^{p(e)}$ is determined by plasticity theory with isotropic hardening employing Mendelson's reformulation of the Prandtl-Reuss Equations in terms of the strain deviators e'_{ij} [9].

$$d\bar{\varepsilon}_{ij}^{p(e)} = \left(\frac{\bar{e}_{ij}{}'}{\bar{e}_{eff}}\right)^{(e)} d\bar{\varepsilon}_{eff}^{p(e)} \text{ where} \tag{17}$$

$$\bar{e}_{eff} = \sqrt{\frac{2}{3}\bar{e}'_{ij}\bar{e}'_{ij}} \text{ and} \tag{18}$$

$$\bar{e}'_{ij} = \bar{\varepsilon}_{ij} - \frac{1}{3\bar{\varepsilon}_{kk}}\delta_{ij} - \bar{\varepsilon}^p_{ij}|_{previous} \, . \tag{19}$$

with $\bar{\varepsilon}^p_{ij}|_{previous}$ being the plastic strains of the previous load step. The effective plastic strain increment is

$$d\bar{\varepsilon}_{eff}^{p(e)} = \bar{e}_{eff}^{(e)} - \frac{\overline{\sigma}_{eff}^{(e)}}{3\mu} \tag{20}$$

where $\overline{\sigma}_{eff}^{(e)}$ is the effective von-Mises stress in the element e. The load history is defined by homogenized strain increment $d\bar{\boldsymbol{\varepsilon}}$, and the subdomain plastic strains are calculated iteratively using the method of successive elastic solutions proposed in Mendelson [9], decomposing uniform subdomain plastic strains in previous and incremental parts

$$\bar{\varepsilon}_{ij}^{p(e)} = \bar{\varepsilon}_{ij}^{p(e)}|_{previous} + d\bar{\varepsilon}_{ij}^{p(e)}. \tag{21}$$

3 Results

The elastoplastic analysis of periodically perforated metal sheets was carried out employing the concepts discussed in the previous sections to analyze the TFA's capabilities. It should be noted that a similar analysis can be seen in Cavalcante and Pindera [10] but for a different numerical approach. All analyzes were performed in a Matlab 2019a environment [11] with an Intel Core i7-7700HQ processor running at 3.80 GHz with 16 GBs of RAM.

The perforated metal sheet presents circular holes distributed in a hexagonal array with a volume fraction of 25%. Discretizations disposes the elements along the angular and radial directions: 30x5 (150 elements) and 90x15 (1350 elements). Figure 1 shows the discretizations for quadrilateral elements.

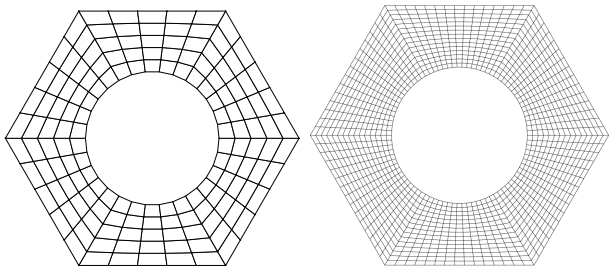

(a) 30x5. (b) 90x15.

Figure 1. Discretizations of the unit cell.

The strain hardening of the aluminum matrix is described by a power-law hardening, which takes the form

$$\sigma_{eff} = \sigma_y + H_p \left(\varepsilon^p_{eff}\right)^n \tag{22}$$

where σ_y is the yield stress, H_p is the strain-hardening slope and n is the exponent of the power-law. Elastic and plastic parameters of the aluminum alloy employed in the perforated sheet studies: $E = 72.7\ MPa$, $\nu = 0.34$, $\sigma_y = 240MPa$, $H_p = 457.589MPa$, $n = 0.4218$.

The study employs linear, quadratic and higher-order quadilateral lagrangian elements for both meshes. The higher-order quadrilateral element is a five-degree Lagrangian interpolation with 36 nodes each. The higer-order element can represent more complex strain fields, delivering better results than the quadratic element with less discretization. However, it is noteworthy that the number of nodes increases significantly. Table 1 shows a comparison between the number of nodes for each of the adopted meshes. With this higher-order element, it was possible to verify the influence of node density per element in the analyses.

Table 1. Number of elements and nodes per discretization.

	Discretizations	
	30x5	90x15
Elements	150	1350
Nodes (Linear Element)	180	1440
Nodes (Quadratic Element)	660	5580
Nodes (Fifth-Order Element)	3900	34200

All models were subjected to periodic boundary conditions and macroscopic loadings to reflect uniaxial tension scenario. The load was applied in 30 equal increment steps until reaching homogeneous strain of 3%. The TFA results are compared with the classical Finite Element Analysis.

The results are presented below considering uniaxial tension scenario, Figure 2. The analyses were carried out as follows: comparing models employing the same finite element but with different mesh discretizations. Thus, the objective was to highlight the influence of the mesh discretization for the same type of finite element and the order of the employed finite element.

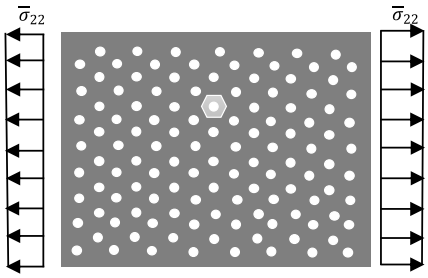

Figure 2. Uniaxial tension.

Figure 3 shows the results of the models with all meshes using the linear, quadratic and high-order elements. The TFA data is compared with classical FEA results.

Table 2 shows the relative differences between the classical FEA and TFA for the same finite element and discretization (number of elements). Because TFA approximates stress/strain fields assuming uniform distribution per element, it was expected that TFA results would converge with FEA results for higher levels of discretization because it can capture the localized plastic strain field. The quadratic finite element presented similar results compared with the fifth-order finite element.

Higher-order finite elements give a less stiff macroscopic response for TFA because they can more correctly capture the localized field when a uniform eigenstrain is imposed per element. For the coarsest meshes, the maximum relative difference was lower than 10% for the macroscopic strain of 3%, and for the most refined meshes, the relative differences were less than 1.5%.

The effective plastic strain and stress distributions are presented for the 90x15 meshes of linear, quadratic, and fifth-order finite elements (Figure 4). These fields present uniform averaged distributions per element to compare the results obtained by classical FEA and TFA approaches more directly. For this level of discretization, the localized response obtained by TFA is as good as the localized response obtained by classical FEA for all the analyzed finite elements.

Also, processing time for all simulations are presented in Table 3. The processing time table can be explained by FEA's and TFA's bottleneck: while the first is the solution of linear systems (which is related with the number of the global degrees of fredom), the latter is summation (which is related with the number of elements).

For linear elements and high level of discretization, the computational cost of the summation is more significant than the solution of the global system of equations. TFA's advantage can be observed for higher-order finite

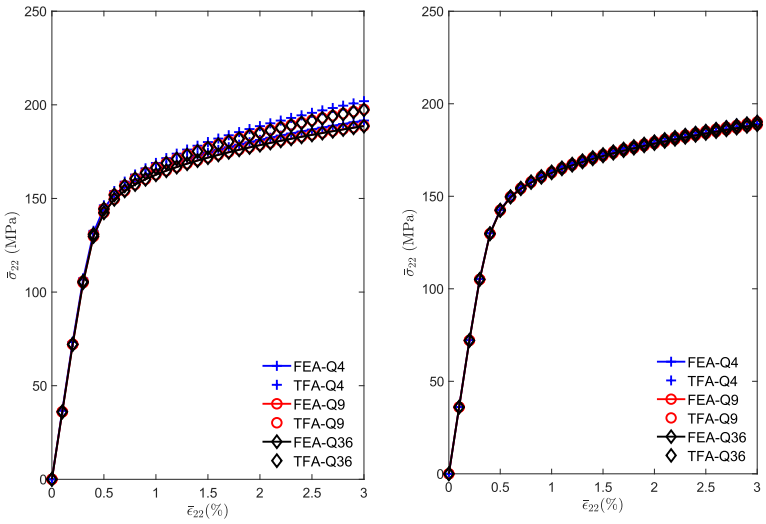

(a) 30x5 (b) 90x15

Figure 3. Macroscopic stress-strain curve for different discretizations.

Table 2. Relative differences between FEA and TFA.

Uniaxial Tension						
Macroscopic Strain	0.5%	1%	1.5%	2%	2.5%	3%
Q4 30x5	1.11%	2.35%	3.26%	4.06%	4.77%	5.40%
Q4 90x15	0.16%	0.40%	0.61%	0.81%	0.98%	1.14%
Q9 30x5	1.42%	2.35%	3.10%	3.70%	4.22%	4.68%
Q9 90x15	0.17%	0.34%	0.49%	0.61%	0.73%	0.83%
Q36 30x5	1.44%	2.28%	3.02%	3.62%	4.13%	4.58%
Q36 90x15	0.18%	0.34%	0.48%	0.60%	0.72%	0.82%

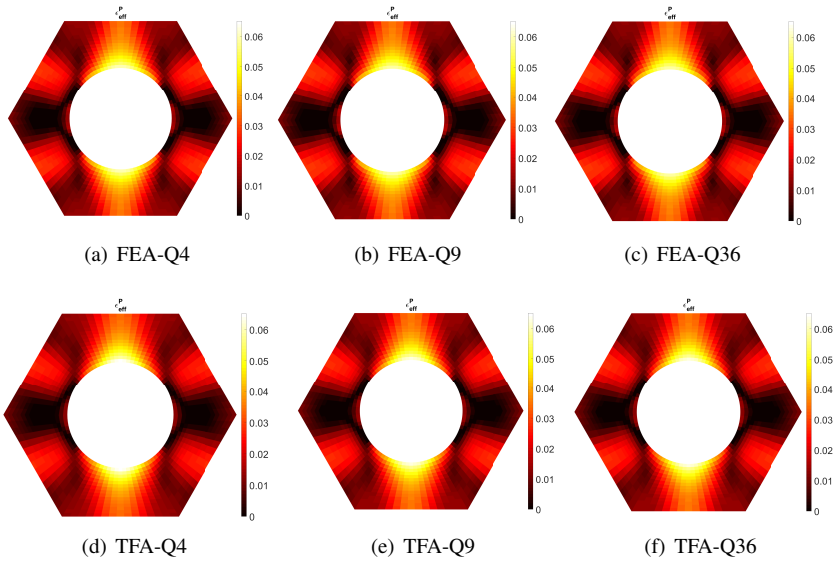

(a) FEA-Q4 (b) FEA-Q9 (c) FEA-Q36

(d) TFA-Q4 (e) TFA-Q9 (f) TFA-Q36

Figure 4. Effective plastic strain field for classical FEA and TFA approaches.

elements when the summation is cheaper than the solution of the global linear system of equations. This fact can be seen in 90x15 discretization using Q36 elements, where TFA's time is much smaller.

Table 3. Processing time for all analysis.

	Q4 30x5	Q4 90x15	Q9 30x5	Q9 90x15	Q36 30x5	Q36 90x15
TFA	49.89	3675.68	39.39	3532.39	21.49	1716.95
FEA	45.42	440.60	80.08	821.66	366.48	6024.10

4 Conclusions

The relationship between the discretization of the mesh and the stiffness of the FEA result is well known. This relation is associated with the element capacity to represent the local deformation: the deformation representation is simplified by decreasing the element size, demanding less from the finite element to represent the local response.

The coupling of TFA with higher-order finite elements improves the concordance with the classical FEA results. However, the employment of higher-order finite elements must be integrated with a suitable discretization of the mesh. The mesh refinement is more critical in obtaining better results with TFA than the application of higher-order finite elements. Best results were achieved for the fifth-order element in 90x15 mesh, where the maximum error was smaller than 1% using less than a third of the time in the analysis.

Thus, capturing the localized plastic strains by a refined mesh is more critical than the tendency to obtain stiffer results due to the limitation of the finite element to represent the local response when a lower-order finite element is employed.

Acknowledgements. The authors would like to acknowledge CNPq financial support.

Authorship statement. The authors hereby confirm that they are the sole liable persons responsible for the authorship of this work, and that all material that has been herein included as part of the present paper is either the property (and authorship) of the authors, or has the permission of the owners to be included here.

References

[1] G. J. Dvorak. Thermal Expansion of Elastic-Plastic Composite Materials. *J. Appl. Mech.*, vol. 53, n. 4, pp. 737–743, 1986.

[2] Y. Benveniste and G. J. Dvorak. On a Correspondence Between Mechanical and Thermal Effects in Two-Phase Composites. In *Micromechanics and Inhomogeneity*, number 1986, pp. 65–81. Springer New York, New York, NY, 1990.

[3] G. J. Dvorak. On uniform fields in heterogeneous media. In *Proc. R. Soc. London A Math. Phys. Eng. Sci.*, volume 431, pp. 89–110. The Royal Society, 1990.

[4] Y. Benveniste and G. J. Dvorak. Some Remarks on a Class of Uniform Fields in Fibrous Composites. *J. Appl. Mech.*, vol. 59, n. 4, pp. 1030–1032, 1992.

[5] G. J. Dvorak. Transformation field analysis of inelastic composite materials. *Proc. R. Soc. London. Ser. A Math. Phys. Sci.*, vol. 437, n. 1900, pp. 311–327, 1992.

[6] G. J. Dvorak, A. M. Wafa, and Y. A. Bahei-El-Din. Implementation of the transformation field analysis for inelastic composite materials. *Comput. Mech.*, vol. 14, n. 3, pp. 201–228, 1994.

[7] A. S. Drago and M.-J. J. Pindera. Micro-macromechanical analysis of heterogeneous materials: Macroscopically homogeneous vs periodic microstructures. *Compos. Sci. Technol.*, vol. 67, n. 6, pp. 1243–1263, 2007.

[8] R. Hill. Elastic properties of reinforced solids: Some theoretical principles. *J. Mech. Phys. Solids*, vol. 11, n. 5, pp. 357–372, 1963.

[9] A. Mendelson. *Plasticity, theory and application*. Robert E. Krieger Publishing Company, Malabar, FL, first edition edition, 1968.

[10] M. A. A. Cavalcante and M.-J. Pindera. Finite-volume enabled transformation field analysis of periodic materials. *Int. J. Mech. Mater. Des.*, vol. 9, n. 2, pp. 153–179, 2013.

[11] The MathWorks Inc. Matlab 2019a, 2019.